



H₂O₂-assisted microwave synthesis of NiO/CNT nanocomposite material for supercapacitor applications

Veeman Sannasi¹ · K. Uma Maheswari¹ · C. Karthikeyan¹ · S. Karuppuchamy¹

Received: 16 November 2019 / Revised: 19 March 2020 / Accepted: 4 April 2020 / Published online: 15 May 2020
© Springer-Verlag GmbH Germany, part of Springer Nature 2020

Abstract

NiO nanoflakes anchored on carbon nanotubes (CNTs) were fabricated through a H₂O₂-assisted microwave irradiation method. The formation of the NiO/CNT nanocomposites were characterised by powder X-ray diffraction (PXRD), Fourier transform infrared spectroscopy (FT-IR), micro Raman spectroscopy and X-ray photoelectron spectroscopy. Surface morphology studies of the prepared materials were carried out using scanning and transmission electron microscopy (SEM and TEM). The electrochemical performance of the NiO and NiO/CNTs were analysed by cyclic voltammetry (CV), galvanostatic charge-discharge (GCD) and electrochemical impedance spectroscopy (EIS) techniques. GCD studies of the NiO/CNTs reveal a maximum specific capacitance of 258 F/g at 1 A/g current density in 2 M KOH aqueous electrolyte was achieved for 1:1 ratio of NiO/CNTs composite. Further, a specific capacitance of 258 F/g at 1 A/g current density obtained for 1:1 ratio of NiO/CNTs is almost 2.15 times higher than that of prepared NiO (120 F/g) which indicates an excellent synergistic effect in NiO/CNTs nanocomposite. Furthermore, the NiO/CNTs nanocomposite electrode showed outstanding cycling stability retention of 86% of the initial capacitance after 2500 cycles.

Keywords Microwave method · NiO/CNT composite · Supercapacitor · H₂O₂

Introduction

The enhanced concern about the rising global warming and increasing energy crises due to population growth triggers the demand for new energy conversion and energy-saving technologies/devices. With the above-said concern, supercapacitors have the considerable interest as a promising energy storage/power supply for electric vehicles due to its fast charging-discharging process, high power density than secondary batteries, high energy delivering than conventional capacitors and excellent cycling stability [1–6]. Based on the energy storage mechanism, a supercapacitor can be divided into two types: (i) electric double-layer capacitor (EDLC) (ionic adsorption and

desorption on the surface of the electrode/electrolyte interfaces) and (ii) pseudocapacitor (oxidation and reduction process occur between the electrode/electrolyte ions) [7–12]. Carbonaceous materials such as activated carbon, carbon aerogel, graphene and carbon nanotubes (CNTs) were used as electrode materials in EDLCs. The above-said carbon-based materials attract in EDLC by their high surface area, non-toxic, low cost and abundance in nature. Albeit carbon-based materials have good electrical conductivity, chemical stability and high porosity; their application in supercapacitor was limited by their low energy density [13–19].

Conversely, pseudocapacitors showed promising high energy density than EDLC due to their faradaic redox mechanism and commonly used pseudocapacitor materials are conducting polymer and transition metal oxides such as RuO₂ [20], MnO₂ [21], CoO [22], Fe₂O₃ [23] and NiO [24, 25] etc. So far used transition metal oxides, the hydrous RuO₂ is one of the best electrode materials for energy storage applications, because of its unique properties like good redox reversibility and brilliant electrochemical properties. The practical application of RuO₂ in supercapacitors is limited owing to the high cost and less abundance in nature.

Electronic supplementary material The online version of this article (<https://doi.org/10.1007/s11581-020-03563-z>) contains supplementary material, which is available to authorized users.

✉ S. Karuppuchamy
skchamy@gmail.com

¹ Department of Energy Science, Alagappa University, Karaikudi, Tamil Nadu 630003, India

Apart from RuO_2 , among the other metal oxides used for charge storage applications, NiO is a very promising material because of its higher theoretical capacitance above 2500 F/g, low cost, tremendous redox reversibility and ease of synthesis. However, NiO suffers from poor electronic conductivity, ionic conductivity and higher volumetric changes during the charge-discharge cycling and lower rate performance in energy storage devices, which hinders the practical applications. To overcome this poor electronic, ionic conductivity and cyclic stability of pseudocapacitor, electrode material like NiO electrode is composite with carbon materials like CNT due to their superior chemical stability, favourable electrical conductivity and high surface area.

Various research groups are focusing on hybrid supercapacitor, which is composed of high conductive, high power density, longer stability EDLC material along with high energy density transition metal oxide [26–35]. This type of hybrid electrode material generates a mutual behaviour due to EDLCs and pseudocapacitance and hence results in good electrochemical activity. Among the different hybrid composition, composition of NiO and CNTs has been effectively made by various methods like a hydrothermal, electrophoretic deposition, chemical bath deposition, etc., and interest for supercapacitor application in earlier reports due to high capacitance, low cost and long cycling stability.

Yu and co-workers reported the preparation of NiO-CNT nanohybrid through atomic layer deposition and achieved a high specific capacitance of 622 F/g at 2 A/g [36]. While Yu et al. reported a specific capacitance of 1177 F/g at 2 A/g current density for NiO nanosheets on CNT prepared by the electroless plating method [37]. Furthermore, Dai and co-workers reported large-scale fabrication and achieved a maximum specific capacitance of 759 F/g at 0.5 A/g for CNTs and porous NiO nanocomposites by chemical conversion method [38]. But all these preparation methods have used difficult reaction parameters such as high operating temperature, working pressure and several steps. Among the various techniques available for the synthesis of composite materials, microwave method has several advantages like uniform particle size distribution, increasing the phase purity of compound, controlled morphology and rapid synthesis time [39, 40].

The synthesis of electrode materials using microwave process is a well-established one, and so many reports are available for the energy storage applications. In our lab, we have synthesised various metal oxides and their composites using the microwave method and used as electrode materials for supercapacitor applications [41, 42]. Herein, we have successfully synthesised NiO/CNT nanocomposite with the assistance of H_2O_2 by facile, cost-effective and time-effective microwave synthesis. The synthesised NiO and NiO/CNT nanocomposites are tested for supercapacitor applications.

Experimental procedure

Materials

Multi-wall carbon nanotubes (CNTs), Nickel(II) nitrate hexahydrate ($\text{Ni}(\text{NO}_3)_2 \cdot 6\text{H}_2\text{O}$), Hydrogen peroxide (30% H_2O_2) and Ammonia solution (25% NH_4OH) were purchased from Sisco Research Laboratories, Pvt. Ltd., India. All chemicals were used as received without any additional further purification.

Synthesis of NiO

Nickel oxide (NiO) was synthesised by a simple microwave irradiation method. Further, 2.9 g of nickel nitrate hexahydrate was dissolved in 60 mL of deionised (DI) water. Nine millilitres of 30% H_2O_2 was added drop-wise to the above magnetically stir solution and continued until the formation of a homogeneous solution. Then 25% of ammonia solution was added to attain the pH around 11. Then the suspension was transferred into domestic microwave oven using 250 mL microwave autoclave and allowed for microwave irradiation at 560 W for 10 min. After the tenure of time, the autoclave was allowed to cool to attain room temperature. The resultant precipitate was filtered, washed with water and ethanol several times to remove any unreacted species and finally dried at 80 °C for 12 h and then calcined at 300 °C for 2 h in air atmosphere.

Synthesis of NiO/CNT nanocomposite

In this full experiment, different ratio of NiO/MWCNT was prepared by using H_2O_2 in the microwave method. In detail, 100 mg of CNTs were dispersed in 20 mL of DI water using sonication for 30 min. A solution of nickel nitrate hexahydrate in DI water and H_2O_2 were stirred until the formation of a homogeneous solution. To the homogeneous solution, the dispersed CNTs solution was added and continued to stir for another 20 min. Finally, the solution was adjusted to pH of 11 using the ammonia solution. Then the resultant mixture was subjected into microwave irradiation at 560 W for 10 min using a domestic microwave oven. Then the autoclave was allowed to attain the room temperature. The obtained precipitate was filtered, washed with water and ethanol repetitively and dried in a hot air oven at 80 °C for 12 h. Finally, the dried powder was calcined at 300 °C for 2 h in air atmosphere. The effect of CNT content in NiO-CNT composite on their electrochemical behaviour was studied by using different ratio such as 1:0.5, 0.5:1, 1:1 of NiO and CNT composite materials. The composite materials were prepared by using the corresponding weight ratio of nickel nitrate hexahydrate and CNT as reactants and the obtained products were denoted as 1: 0.5, 0.5:1 and 1:1 respectively.

Characterisation

The phase formation and crystal structure of the prepared NiO-CNT composites were characterised by powder X-ray diffraction (X'pert PRO analytical diffractometer) using Cu K α as radiation (1.541 Å) source. The metal-oxygen vibration modes of composite samples were confirmed through FT-IR spectroscopy and were recorded using Fourier transform infrared spectrophotometer employing Thermo Nicolet 380. Raman active modes of NiO and all composite materials were analysed using Imaging Spectrograph STR 500 nm focal length laser micro Raman spectrometer SEKI, Japan, with resolution 1/0.6 cm⁻¹/pixel and Flat Field 27 mm (W) × 14 mm (H). PHI-VERSAPROBE III-X-ray photoelectron spectroscopy were used for measure the elemental composition and chemical states of the samples. Scanning electron microscopy (ZEISS-V80) and transmission electron microscopy (JEOL-2100 + high-resolution transmission electron microscope) with an accelerating voltage of 200 kV and resolution point of 0.194 nm were used to study the morphology of the synthesised samples.

Electrochemical measurements

The electrochemical behaviours of the NiO/CNT composites prepared by microwave irradiation method were characterised using Biologic science instruments (SP-200) in the three-electrode configuration. A three-electrode system which consists of the active material coated Ni-foam, Ag/AgCl and a platinum wire was utilised as a working, reference and counter electrodes respectively. The Ni foam (1 × 1 cm) was pre-treated using 3 M HCl under sonication for 15 min followed by washing with acetone, ethanol and water. The slurry was prepared using an active material (NiO/CNT), acetylene black and polyvinylidene difluoride in the weight ratio of 85:10:5 and *N*-methyl-2-pyrrolidone as a solvent. The slurry was coated on the pre-treated Ni-foam and dried at 80 °C for 12 h. The electrochemical studies such as cyclic voltammetry (CV), galvanostatic charge-discharge studies (GCD) and electrochemical impedance spectroscopy (EIS) were conducted using 2 M KOH aqueous solution as the electrolyte.

Results and discussion

The NiO/CNT composites were prepared by H₂O₂-assisted microwave irradiation method using the nickel nitrate hexahydrate as the starting material. Scheme 1 shows the preparation of NiO/CNT composites. Nickel nitrate hexahydrate in DI water solution was slowly added to prior purified and dispersed MWCNT in DI water with uniform stirring. Ammonia solution was added to MWCNT-Ni(NO₃)₂·6H₂O, and finally, 560 W microwave was irradiated for 10 min gave

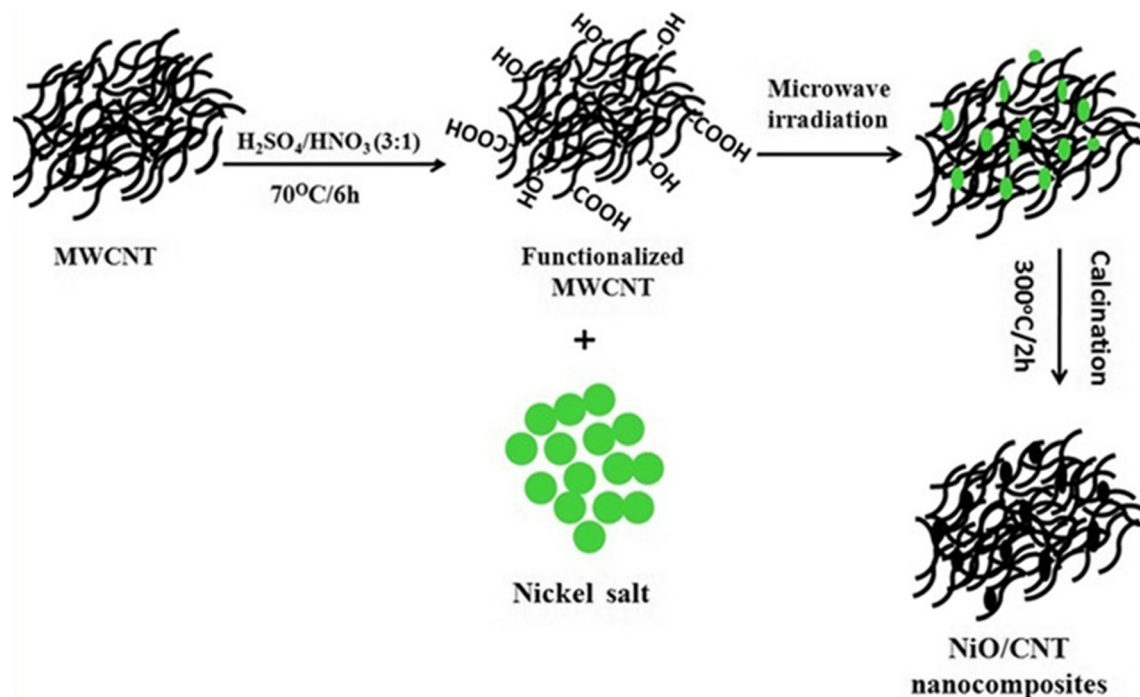
MWCNT/Ni(OH)₂. MWCNT/Ni(OH)₂ was calcined at 300 °C for 2 h in air atmosphere and gave NiO/CNT composite. Further, different ratios of NiO/CNT were prepared by changing the amount of Ni salt and CNT.

XRD analysis

The crystal structure and phase formation of the annealed materials were analysed by powder X-ray diffraction (PXRD), and the results are shown in Fig. 1. XRD patterns of the prepared NiO and NiO/CNT nanocomposites (Fig. 1a–d) indicate the formation of the nanocomposite. The XRD of the prepared NiO showed diffraction peaks at 2 θ value of 37.3°, 43.5°, 62.3°, 75.4° which are attributed to the (111), (200), (220) and (222) crystal planes. The presence of (111), (200), (220) and (222) crystal planes, thus well matched to the NiO cubic system in Fm3m spatial group (JCPDS No-78-0643), confirms the formation of phase pure NiO [38]. While, the prepared NiO/CNT composites showed all the above-said diffraction peaks of NiO along with a new diffraction peak at 26.5°. The existence of new diffraction peak at 26.5° could be perfectly indexed to the plane (002) of a graphitic form CNTs. Further, the variation of NiO/CNT ratio was concurred by the difference in plane intensity corresponding to the NiO and shown in Fig. 1b–d. Moreover, the absence of any other impurity peaks indicates that the synthesised NiO and NiO/CNT composites are high phase purity.

FT-IR analysis

Figure 2a–d shows the FT-IR spectra of pure NiO and NiO/CNTs composites. In the FT-IR spectrum of NiO, peaks at around 3422, 2922, 2854, 1587, 1023, 707 and 463 cm⁻¹ were observed. While, the FT-IR spectra of NiO/CNT composites showed all the above peaks which observed for NiO along with new peaks at 2342 and 1625 cm⁻¹. A broad band at 3422 cm⁻¹ may be attributed to the OH groups of absorbed moisture on the samples during the measurements and OH groups of hydroxyl or acidic groups of MWCNT. Generally, the stretching vibrations of hydroxyl (OH- ions) groups appeared in the high-frequency region at 3200 to 3650 cm⁻¹ [43]. The stretching vibrations at 2922, 2854 and 1427 cm⁻¹ correspond to the C-H symmetric, asymmetric stretching and bending mode. Particularly in Fig. 2c, NiO/CNT composite of 0.5:1 ratio shows a band at 2342 cm⁻¹ which is the -CH₂ and C-CH₃ stretching vibration of defect sites of the CNTs because of the higher amount of CNTs in sample (c). The band at 1625 and 1587 cm⁻¹ attributed to the stretching vibrations of C=C and -C \equiv C respectively, which related to the carbon skeleton of MWCNT. The bands at 1383 and 1023 cm⁻¹ corresponds to the graphite-like tangential mode and the sp³ hybridised carbon in the nanotube walls and C-O stretching vibration.



Scheme 1 Preparation of NiO/CNT nanocomposites

The peaks at 400 to 900 cm^{-1} observed for all the materials indicate the presence of metal oxide (M-O) bond [44–47]

Raman studies

Figure 3a–d represents the Raman spectra of prepared NiO and NiO/CNTs composites. In Fig. 3a, the broad peak observed in the region of around 510 cm^{-1} is attributed to the modes of crystalline Ni-O lattice vibration. The broadened peaks at about 1347, 1575 and 2696 cm^{-1} in Fig. 3b–d

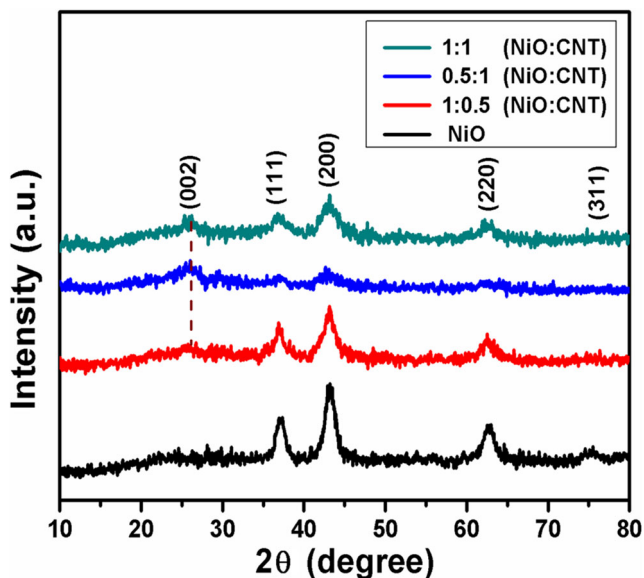


Fig. 1 XRD pattern of NiO (a) and different ratio of NiO/CNT nanocomposites [1:0.5 NiO/CNT (b), 0.5:1 NiO/CNT (c) and 1:1 NiO/CNT (d)]

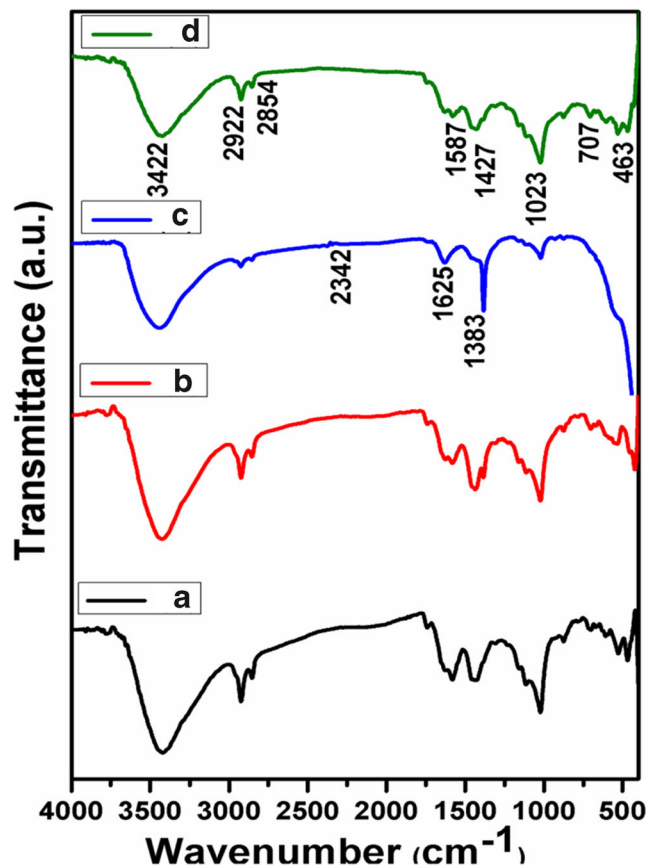


Fig. 2 FT-IR spectra of a NiO, b 1:0.5 NiO/CNT, c 0.5:1 NiO/CNT and d 1:1 NiO/CNT nanocomposites

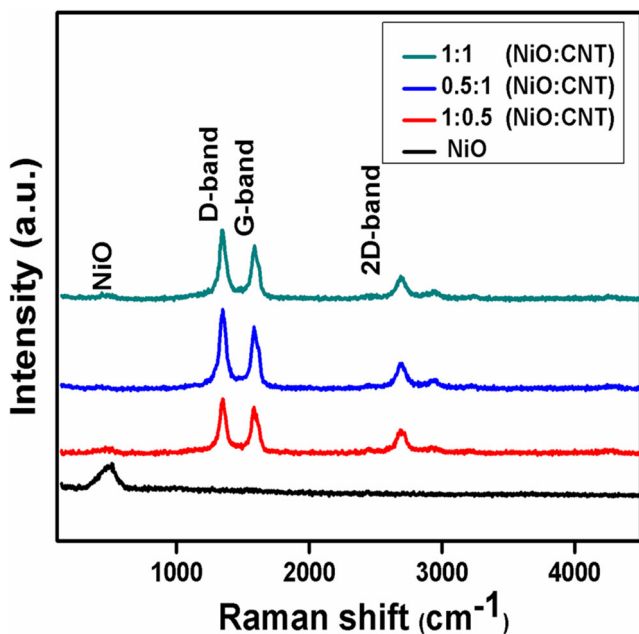


Fig. 3 Raman spectra of a NiO, b 1:0.5 NiO/CNT, c 0.5:1 NiO/CNT and d 1:1 NiO/CNT nanocomposites

correspond to the D, G and 2D bands of CNTs, respectively [48, 49]. The presence of the characteristic peaks of NiO and CNTs in the Raman spectra of NiO/CNT composites indicates that the hybrids are composed of the CNTs and NiO nanoflakes

X-ray photoelectron spectroscopy

Figure 4a–d illustrates the X-ray photoelectron spectra of 1:1 ratio of NiO/CNT nanocomposites. From the XPS spectra, the chemical oxidation state and composition of the samples can be measured. The survey spectrum of the NiO/CNT composites is shown in Fig. 4a. The figure shows the presence of three significant peaks corresponding to the carbon (C 1s), oxygen (O 1s) and nickel (Ni 2p). In Fig. 4b, two main peaks were located at the binding energies of 855.7 eV and 873.4 eV and are ascribed to the Ni 2p_{3/2} and Ni 2p_{1/2} respectively. Besides, two satellite peaks are observed at 861.8 eV and 879.9 eV which is in good agreement with the previously reported literature [36, 50]. Figure 4c shows the C 1s spectrum of NiO/CNT nanocomposites. It shows three peaks positioned at

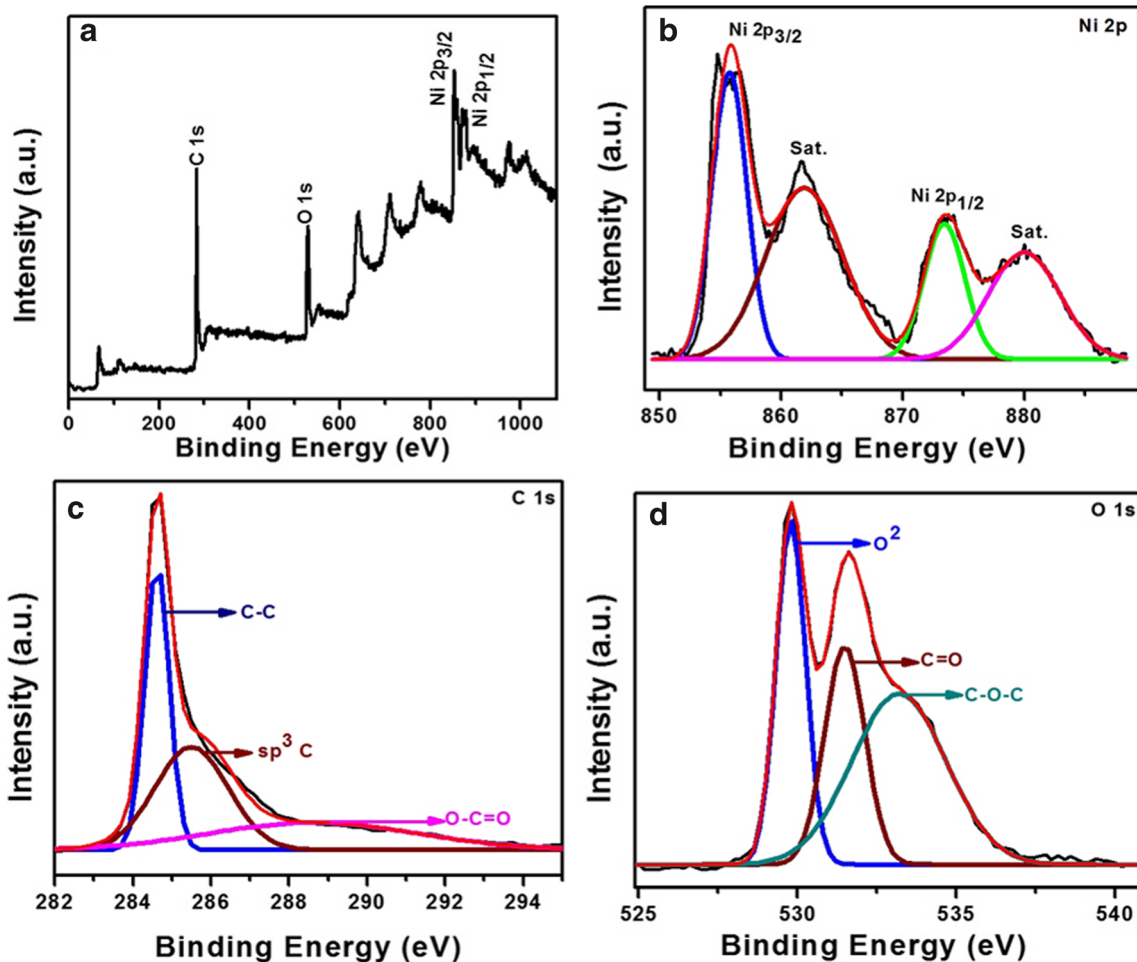


Fig. 4 XPS spectra of a survey spectrum, b Ni 2p, c C 1s and d O 1s of 1:1 NiO/CNT nanocomposites

284.6 eV, 285.4 eV and 288.6 eV which are attributed to C-C graphitic Sp^2 nature of CNTs, C-C atoms with Sp^3 and (O-C=O) respectively. From Fig. 4d, the O 1s spectrum indicates that the three peaks located in the region of 529.7 eV, 531.5 eV and 533.1 eV are attributed to the presence of O^{2-} in NiO lattice, C=O and C-O-C band respectively [36, 51–53]

Surface morphology studies

Scanning electron microscopy and high-resolution transmission electron microscopy were used to demonstrate the morphological and structural characterisation of the synthesised NiO and NiO/CNTs nanocomposites. SEM images of prepared NiO and NiO/CNTs nanocomposites are shown in Fig. 5a–d. SEM analysis further reveals that the prepared NiO has nanoflakes in bundled shape morphology. While, change in morphology was observed for the NiO/CNT composites due to incorporation of carbon nanotubes with NiO nanoflakes and shown in Fig. 5b–d. In particular, Fig. 5b indicates clearly visible nanoflakes due to the lower amount of CNTs in the composite. On the contrary to 1:0.5 ratio of NiO/CNT composite, in 0.5:1.0 ratio of NiO/CNT composite, the CNTs are clearly seen and shown in Fig. 5c. While, the composite of an equal ratio of NiO and CNT (1:1) shows the uniform blend of nanoflakes and CNTs. The formation of a

uniform blend of CNTs and NiO are due to the synergistic mixture of NiO and CNTs, thus further lowers the aggregation. This synergistic effect in 1:1 ratio of NiO and CNTs makes the possibility of the transportation of ions to the active material which favours for energy storage applications.

HR-TEM images and selected area electron diffraction (SAED) pattern were used to illustrate the nanostructure and crystallinity of the prepared 1:1 ratio of NiO/CNTs composites and is given in Fig. 6. TEM images of the 1:1 ratio of NiO/CNTs demonstrate the uniform distribution of NiO nanoflakes (inset in Fig. 6a) across the MWCNTs. Furthermore, the TEM image clearly indicates the formation of flakes like NiO in the lateral size of around 100 nm and aggregation of NiO nanoflakes in the composite. Moreover, TEM images reveal that the diameter of the MWCNT is approximately 10 nm which well connects the NiO nanoflakes.

In Fig. 6c HR-TEM images, the d-spacing values are measured and found to be 0.24 nm and 0.34 nm which corresponds to the (111) and (002) planes of cubic NiO and CNT, respectively [10, 54]. These results are well matched with the XRD results. Furthermore, the selected area electron diffraction (SAED) pattern in Fig. 6d shows the diffraction rings from the inner side to outer side which are well-matched with the (002) plane of CNT and (111), (200), (220), (311) and (222) planes of polycrystalline NiO [13].

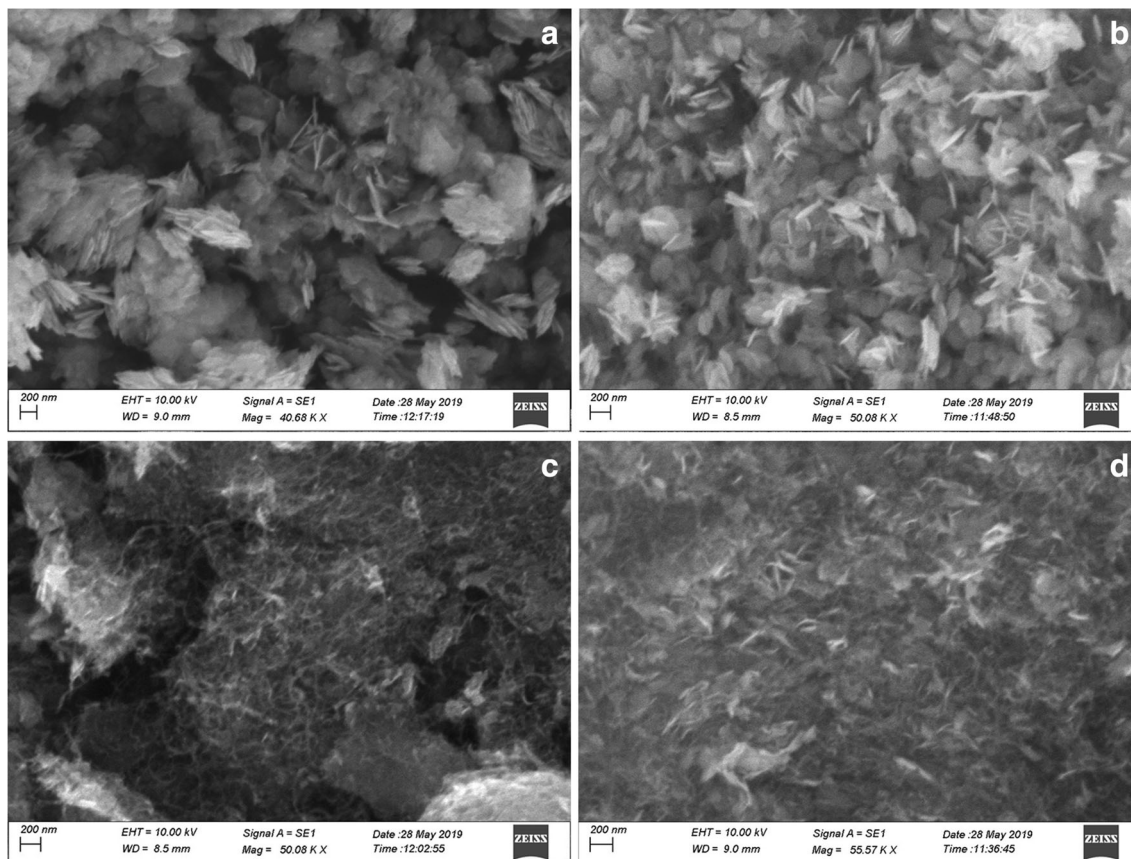


Fig. 5 SEM images of **a** NiO, **b** 1:0.5 NiO/CNT, **c** 0.5:1.0 NiO/CNT and **d** 1:1 NiO/CNT nanocomposites

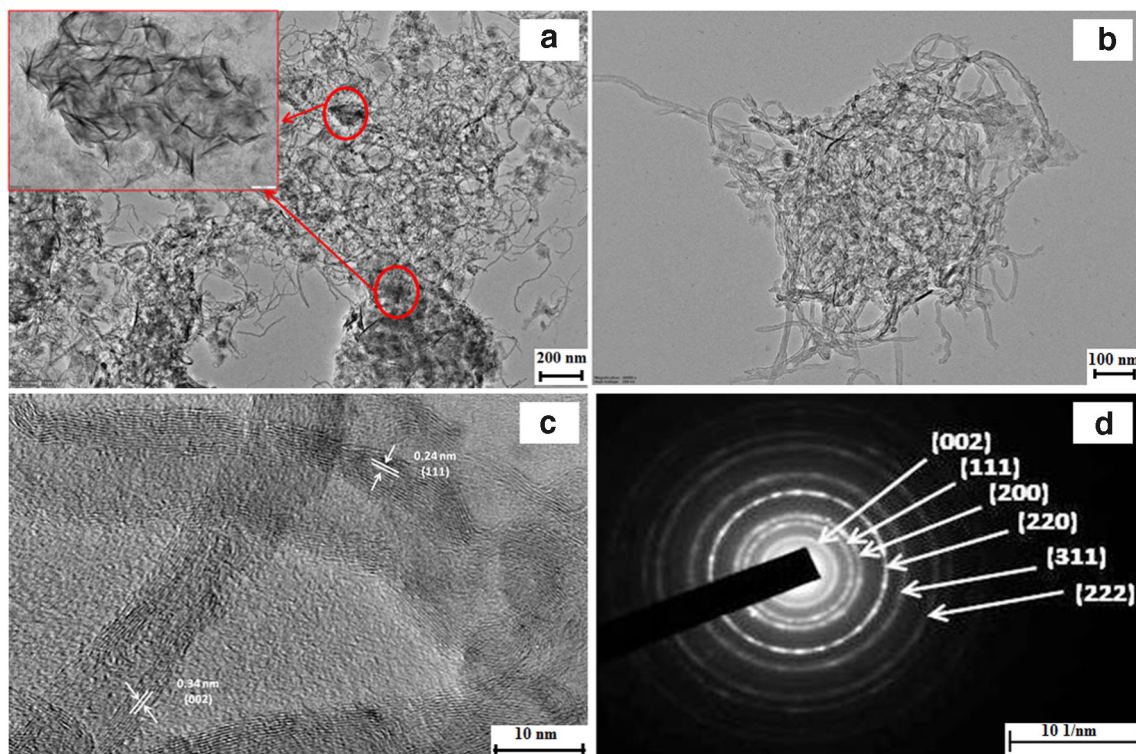


Fig. 6 TEM (a and b), HR-TEM image (c) and the SAED pattern (d) of 1:1 NiO/CNT nanocomposites

This type of connectivity of NiO through the CNT exhibits the good electrical conductivity which causes a good electrochemical response of 1:1 NiO/CNT over the other NiO/CNT ratio and pristine NiO and CNTs

Electrochemical studies

Cyclic voltammetry

The electrochemical behaviour of the prepared NiO and NiO/CNT nanocomposite materials were investigated by cyclic voltammetry studies in an aqueous 2 M KOH electrolyte solution. Figure 7 shows the comparison of cyclic voltammetry curves of CNT, NiO and NiO/CNT (1:1) composite electrode materials in the voltage range of 0 to 0.5 V at 5 mV/s scan rate. As displayed in the Fig. 7, a superior current response is achieved for 1:1 composite of NiO/CNT than the single CNTs and NiO materials indicating the high specific capacitance of NiO/CNT composite. The cyclic voltammogram of CNT was given in supporting information (SI.1).

Cyclic voltammograms of NiO and NiO/CNT composite in different ratios (1:0.5, 0.5:1, 1:1) as electrode materials at scan rates ranging from 5 to 100 mV/s is given in Fig. 8. CV curves of all the NiO and NiO/CNT composite electrode materials showed redox peaks in the anodic and cathodic region, indicating the pseudocapacitive behaviour of NiO and NiO/CNT

composites. Further, enhancement of current and shift in redox peak position was observed for all the electrode materials when increasing the scan rates from 5 to 100 mV/s, which was attributed to increasing of charge mobility [51]. The redox peaks in the electrode materials are ascribed to the oxidation-reduction reactions of NiO/NiOOH and given in

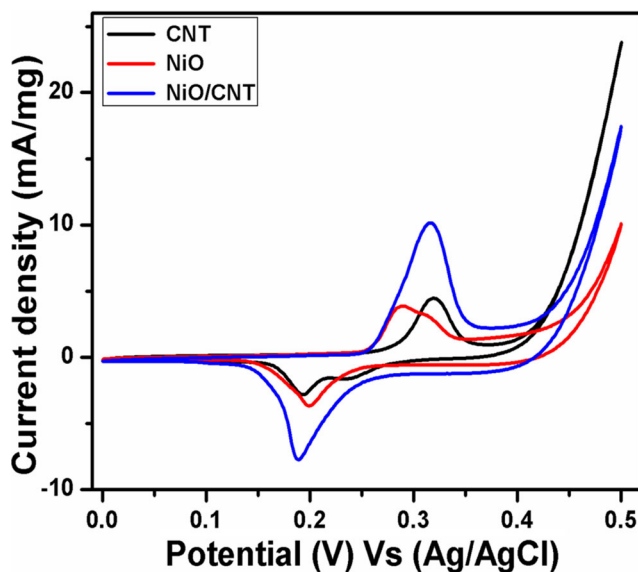


Fig. 7 Cyclic voltammograms (CV) of the prepared NiO, CNT and NiO/CNTs nanocomposites at 5 mV s⁻¹ scan rate in 2 M KOH

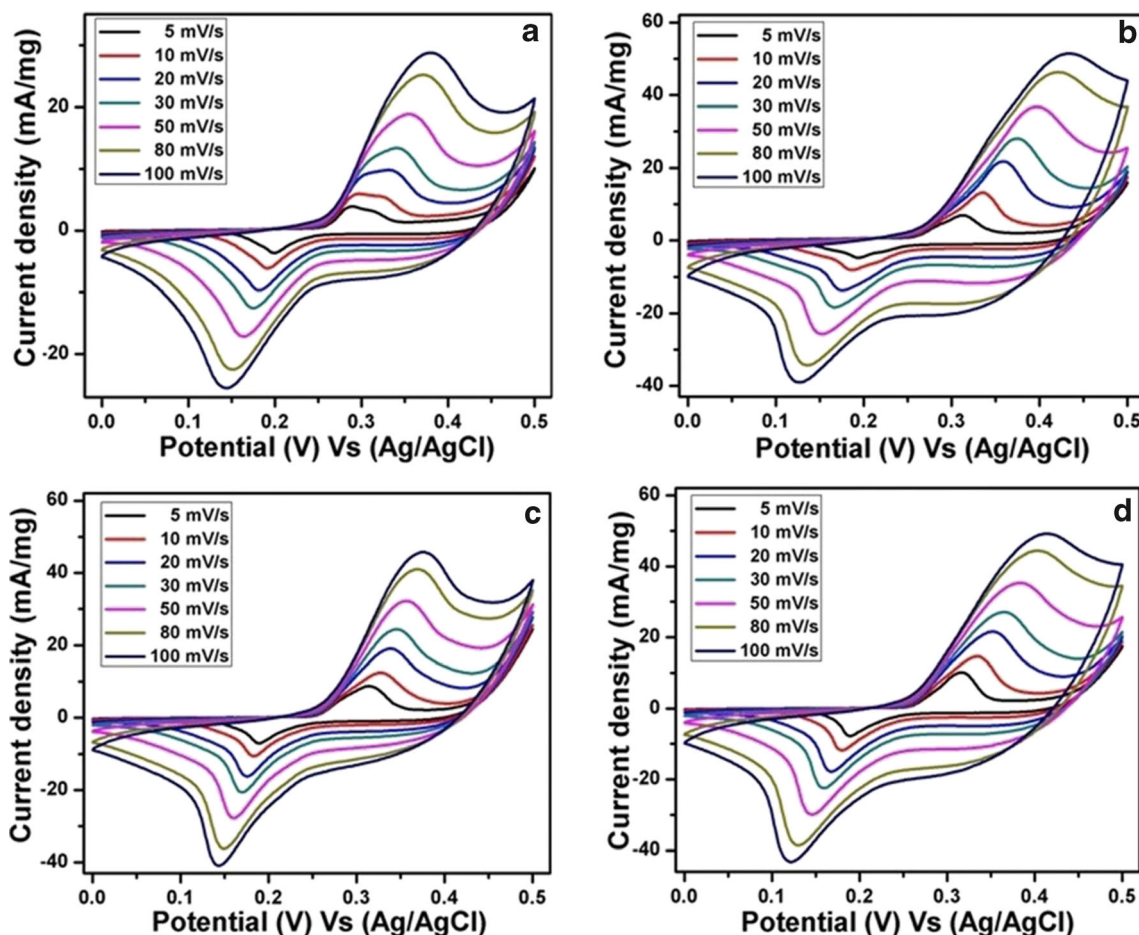


Fig. 8 CV curves of **a** NiO, **b** 1:0.5 NiO/CNT, **c** 0.5:1 NiO/CNT and **d** 1:1 NiO/CNT nanocomposites at different scan rates ranging from 5 to 100 mV s⁻¹

Eq. (1); the anodic peaks are initiated from the oxidation of NiO to NiOOH and the cathodic peaks from reverse reactions [10].



At very low scan rates, the hydroxyl (OH⁻) ions of electrolyte have enough time to intercalate into the electrode material. While, at high scan rates, it is impossible to well intercalate due to minimum time for the diffusion of ions. The enhanced current value is observed for all the composite materials other than NiO material. Especially, 1:1 ratio of NiO/CNT shows high current values than the composites of other ratios such as 1:0.5 and 0.5:1, which is higher compared to NiO electrodes. The equal proportions of the NiO and CNT sample could stimulate the higher amount of dispersion of ions from the aqueous electrolyte solution to the NiO/CNT electrode material, and thus the peak current was increased. These results reveal that carbon nanotube and inorganic NiO take part in a crucial role in energy storage applications [52, 55, 56].

Galvanostatic charge discharge studies

To further investigate the electrochemical characteristics of the prepared NiO and NiO/CNT electrode materials, a

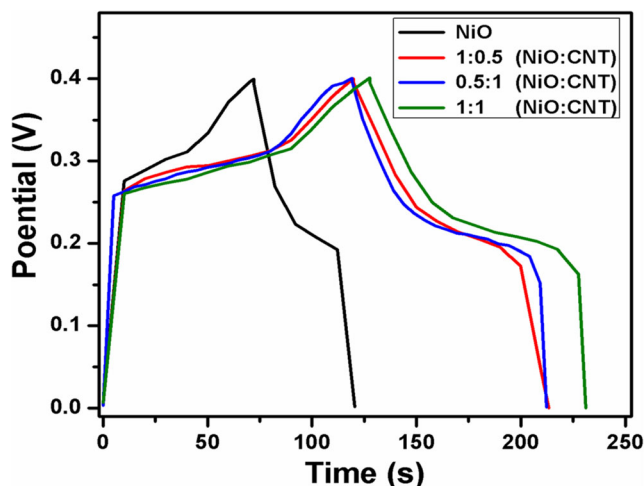


Fig. 9 Galvanostatic charge-discharge (GCD) curves of **a** NiO, **b** 1:0.5 NiO/CNT, **c** 0.5:1 NiO/CNT and **d** 1:1 NiO/CNT at 1 A/g current density in 2 M KOH

galvanostatic charge-discharge test was carried out in the potential range from 0.0 to 0.4 V (vs. Ag/AgCl) in 2 M aqueous KOH electrolyte solution. Figure 9 shows the comparative charge-discharge curves of all the electrode materials at 1 A/g current density. The comparative studies further reveal that the discharging time is high for 1:1 ratio of NiO:CNT nanocomposites compared to other NiO:CNT nanocomposites and NiO. Figure 10a–d illustrates the GCD curves of the NiO and NiO/CNTs nanocomposites at various current densities ranging from 1 to 10 A/g. In all the charge-discharge cycles, an apparent voltage plateau is visible that confirms the pseudocapacitance behaviour of the prepared electrode materials. Furthermore, dissimilarity in the charging and discharging curves of individual electrode material indicates that the materials have pseudocapacitance nature with a small IR drop. The same trend is observed for all the electrode materials.

The specific capacitance of the electrode materials can be calculated from the discharge curves, according to the following Eq. (2).

$$C_{sp} = I \Delta t / m \Delta V \tag{2}$$

Where C is the specific capacitance, I is the current during the discharging process, t is the discharging time (s), m is the

mass of active materials and ΔV is the potential window respectively [57]. From the discharging time of the material and the subsequent calculation of specific capacitance using the above equation, a high specific capacitance of 258 F/g at 1 A/g was achieved for 1:1 NiO/CNT composite electrodes. While, the specific capacitance of 234, 232 and 120 F/g at 1 A/g current density was achieved for 1:0.5, 0.5:1.0 ratio of NiO/CNT composites and NiO respectively. In the GCD studies, the high specific capacitance of 258, 238, 221, 208, 197 and 162 F/g at 1, 2, 3, 4, 5 and 10 A/g was achieved for 1:1 ratio of NiO/CNTs composite electrode. While, NiO electrode material shows specific capacitance of 120, 102, 94, 86, 81 and 65 F/g at 1, 2, 3, 4, 5 and 10 A/g. The high specific capacitance of 1:1 NiO/CNT composite than other NiO/CNT composites (1:0.5 and 0.5:1.0) and NiO indicates that uniform distribution of equally mixed NiO nanoflakes and MWCNT without any self-aggregation favours synergic effect that enhances the high migration of ions into the electrode-electrolyte interface. GCD curves of CNT are given in supporting information (SI.2).

Current density vs. specific capacitance of the prepared electrode materials is shown in Fig. 11a. It can be seen that the specific capacitance of NiO and NiO/CNTs composite electrode materials gradually decreases when increasing the current densities. The decrease of specific capacitance at high

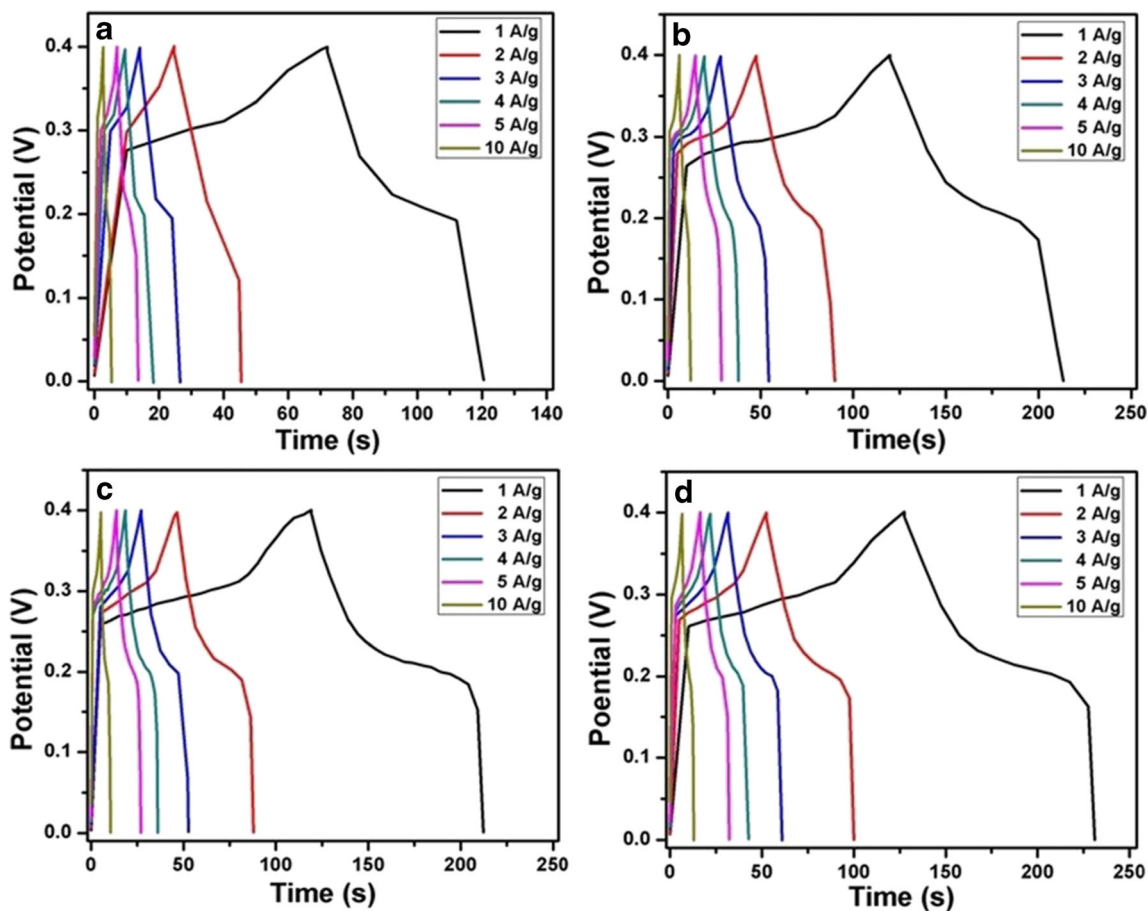


Fig. 10 GCD curves of a NiO, b 1:0.5 NiO/CNT, c 0.5:1 NiO/CNT and d 1:1 NiO/CNT at different current densities ranging from 1 to 10 A/g

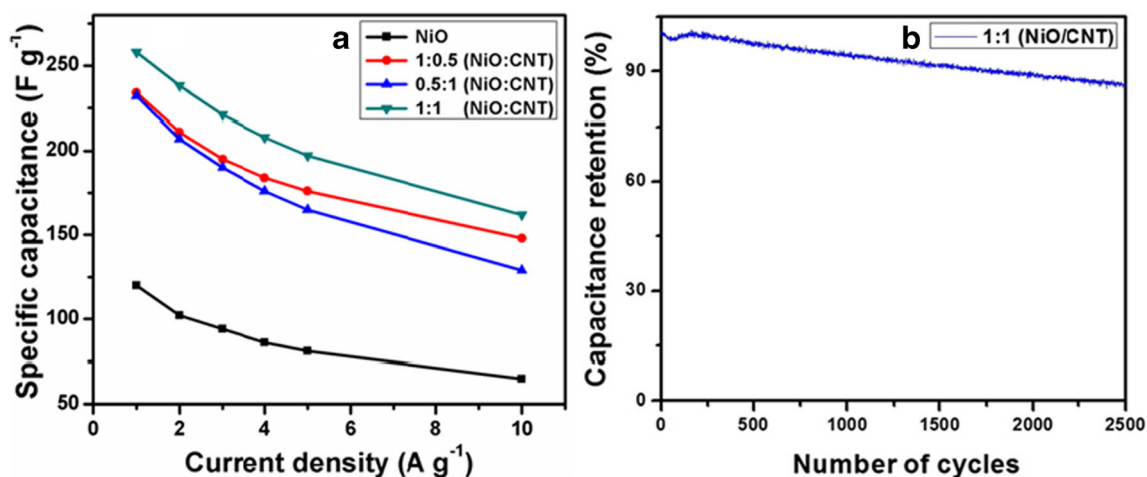


Fig. 11 Change of specific capacitance with discharge current density for the prepared electrode materials **a** and cycling stability of 1:1 NiO/CNT at 6 A/g current density for 2500 cycles

current density is due to the lacking time of redox reaction processes at high current density.

Furthermore, in these NiO/CNT composite materials, the presence of CNTs gives good conducting pathway, and the NiO nanoflakes support the migration of ions into the electrolyte to the electrodes during the charging-discharging process. Also, the stability of the NiO/CNT composite electrode is performed to study the viability of the electrode materials for commercial

applications and given in Fig. 11b. The cyclic stability performance of the NiO/CNT composite electrode shows 86% capacitance retention after 2500 charge-discharge cycles at 6 A/g current density which indicates the excellent durability of the 1:1 ratio of NiO/CNT composite electrode. The specific capacitance of the 1:1 ratio of NiO/CNT composite electrode is compared to other NiO and CNT-Ni-based composite electrode materials and given in Table 1.

Table 1 Capacitive performance of NiO and some carbon materials with Ni-based electrodes

S. No	Type of materials	Specific capacitance (F/g)	Electrolyte	Stability	Reference
1.	NiO nanosheet	81.67 at 0.5 A/g	3 M KOH	78.5% after 3000 cycles at 0.5 A/g	[25]
2.	NiO nanoflakes	137.7 at 0.2 A/g	2 M KOH	91.6% after 1000 cycles at 0.2 A/g	[58]
3.	Carbon-based NiO hollow spheres (C@NiO HSs)	211 at 1 A/g	6 M KOH	84.6% after 1000 cycles at 5 A/g	[59]
4.	Carbon-coated nickel oxide nanofibers	288 at 0.3 A/g	1 M KOH	89% after 3000 cycles at 0.3 A/g	[60]
5.	NiCo ₂ O ₄ /CNTs doped carbon nanofibers	220 at 1 A/g	1 M KOH	–	[61]
6.	NiO nanostructure on nickel foam	250 at 0.5 A/g	2 M KOH	75% after 2000 cycles at 0.5 A/g	[62]
7.	NiO nano powder	200	1 M KOH	–	[63]
8.	NiO-AC	248 at 1 A/g	6 M KOH	98.2% after 1000 cycles at 2 A/g	[64]
9.	Porous nickel oxide-carbon nanotubes	245 at 1.11 A/g	1 M KOH	64.3% retention after 300 at 1 A/g	[65]
10.	Nickel oxide/CNT nanocomposite	160 at 10 mA/g	2 M KOH	–	[66]
11.	Porous MWCNTs–NiO composite	206 at 0.1 A/g	2 M KOH	89% after 200 cycles at 2 A/g	[67]
12.	NiO (microwave method (M.W), high temperature solid state method (HTSS))	MW-186 at 2 mA/cm ² , HTSS-97 at 2 mA/cm ²	6 M KOH	91.4%, 76.7% after 1000 cycles at 2 mA/cm ²	[68]
13.	NiO nanoflakes/graphene	240 at 5 A/g	6 M KOH	100% specific capacity after 1500 cycles at 5 A/g	[69]
14.	NiO thin films	167 at 5 A/g	2 M KOH	–	[70]
15.	Mesoporous nickel oxide	124 F/g	3 wt.% KOH	–	[71]
16.	NiO nanowall arrays	270 F/g at 0.67 A/g	1 M KOH	93% after 4000 cycles at 13.5 A/g	[72]
17.	NiO/CNTs/carbon cloth	162.41 at 0.5 mA	1 M KOH	100 cycles	[73]
18.	NiO/CNTs	258 F/g at 1 A/g	2 M KOH	86% after 2500 cycles at 6 A/g	This work

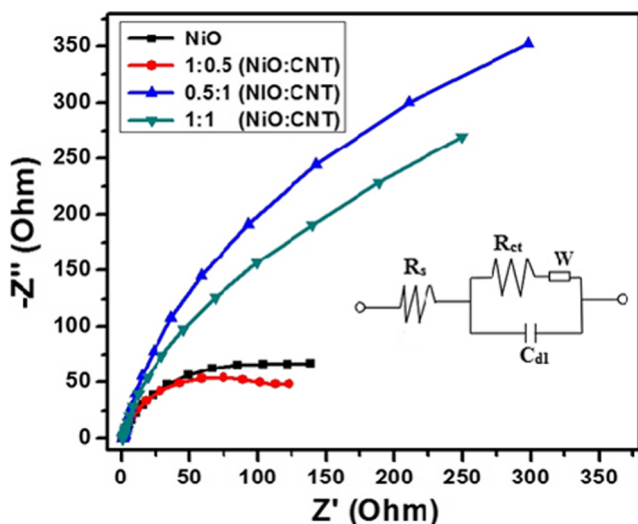


Fig. 12 Nyquist plots of **a** NiO, **b** 1:0.5 NiO/CNT, **c** 0.5:1 NiO/CNT and **d** 1:1 NiO/CNT nanocomposites in 2 M KOH with the amplitude of 10 mV in the frequency range from 200 kHz to 100 mHz by using a Pt wire as the counter electrode and Ag/AgCl as the reference electrode

EIS studies

Charge transfer kinetics of the pure NiO and various ratios of the NiO/CNT composites were studied by using electrochemical impedance (EIS) spectroscopy. EIS measurements also conducted in the frequency ranges from 200 kHz to 0.1 Hz in the amplitude range of 10 mV. As shown in Fig. 12, in all the electrodes, the Nyquist plots consist of an incomplete semicircle area in high-frequency region, indicating that the interfacial charge transfer resistance (R_{ct}) and the vertical line in the lower frequency region, referring to the Warburg resistance (W_d), represents the electrolyte ions in diffused level. The resistance of the NiO/CNT electrodes is much smaller than the pure NiO electrode (R_s values 0.79, 0.95, 0.98 and 1.07 corresponds to the 1:1, 1:0.5, 0.5:1 ratios of NiO:CNT and NiO). It denotes excellent capacitive behaviour. The equivalent circuit was obtained and presented the inset of the figure. The electrical conductivity of the NiO electrode is slightly improved by adding the CNTs. From these experiment results, the 1:1 ratios of NiO/CNT composite electrode are the right choice for high diffusion of ions in aqueous electrolytes. These EIS results are in good agreement with CV and GCD results. Based on the results, the NiO/CNTs composites can be a high capacitive electrode material for energy storage applications.

Conclusion

In summary, we have successfully prepared NiO/CNTs nanocomposite using microwave irradiation method with the assistance of H_2O_2 . The structure of the composite, surface morphology and electrochemical behaviour of NiO/CNTs

nanocomposites were investigated. The synthesised NiO/CNTs nanocomposite electrodes achieved an excellent specific capacitance of 258 F/g at a current density of 1 A/g and showed high stability. The composite material retained an 86% of their initial capacitance even after 2500 charge-discharge cycles. These nanocomposite materials efficiently boost the electrical conductivity of the electrode and thus increase the cyclic stability of the materials. From the above considerations, this effective synergistic material is beneficial for electrochemical storage devices.

Acknowledgements The authors express their sincere thanks to MHRD-RUSA, Government of India and Ministry of Higher Education, Government of Tamil Nadu, RUSA R&I-Phase-I component 8.0 and RUSA-Phase 2.0 grant sanctioned vide Letter No. F.24-51/2014-U, for financial support. The authors gratefully acknowledge DST, New Delhi, for providing partial financial support to carry out this research work under DST-PURSE scheme. Dr. V. Sannasi gratefully acknowledges the Council of Scientific and Industrial Research (CSIR), Government of India for providing CSIR-RA.

Supporting information Supporting information of this manuscript is available from the electronic format.

Compliance with ethical standards

Conflict of interest The authors declare that they have no conflict of interest.

References

- Chen N, Zhou J, Zhu G, Kang Q, Ji H, Zhang Y, Wang X, Peng L, Guo X, Lu C, Chen J (2018) A high-performance asymmetric supercapacitor based on vanadyl phosphate/carbon nanocomposites and polypyrrole-derived carbon nanowires. *Nanoscale* 10(8):3709–3719
- Mirzaeian M, Abbas Q, Ogwu A, Hall P, Goldin M, Mirzaeian M, Jirandehi HF (2017) Electrode and electrolyte materials for electrochemical capacitors. *Int J Hydrog Energy* 42(40):25565–25587
- Zhang X, Yan P, Zhang R, Jin J, Xu J, Wu C, Liu H (2016) Fabrication of graphene and core-shell activated porous carbon-coated carbon nanotube hybrids with excellent electrochemical performance for supercapacitors. *Int J Hydrog Energy* 41(15):6394–6402
- Afzal A, Abuilaiwi FA, Habib A, Awais M, Waje SB, Atieh MA (2017) Polypyrrole/carbon nanotube supercapacitors: technological advances and challenges. *J Power Sources* 352:174–186
- Gao YP, Zhai ZB, Huang KJ, Zhang YY (2017) Energy storage applications of biomass-derived carbon materials: batteries and supercapacitors. *New J Chem* 41(20):11456–11470
- Liu S, Li S, Sekar K, Li R, Zhu Y, Xing R, Nakata K, Fujishima A (2019) Hierarchical ZnS@C@MoS₂ core-shell nanostructures as efficient hydrogen evolution electrocatalyst for alkaline water electrolysis. *Int J Hydrog Energy* 44(47):25310–25318
- Tseng LH, Hsiao CH, Nguyen DD, Hsieh PY, Lee CY, Tai NH (2018) Activated carbon sandwiched manganese dioxide/graphene ternary composites for supercapacitor electrodes. *Electrochim Acta* 266:284–292

8. Kumar RD, Karuppachamy S (2016) Microwave mediated synthesis of nanostructured CoWO_4 and CoWO_3 for supercapacitor applications. *J Alloys Compd* 674:384–391
9. Liu P, Yan J, Gao X, Huang Y, Zhang Y (2018) Construction of layer-by-layer sandwiched graphene/polyaniline nanorods/carbon nanotubes heterostructures for high performance supercapacitors. *Electrochim Acta* 272:77–87
10. Lai H, Wu Q, Zhao J, Shang L, Li H, Che R, Lyu Z, Xiong J, Yang L, Wang X, Hu Z (2016) Mesoporous NiO/Ni composites for high-performance electrochemical energy storage. *Energy Environ Sci* 9(6):2053–2060
11. Nunes WG, Da Silva LM, Vicentini R, Freitas BG, Costa LH, Pascon AM, Zanin H (2019) Nickel oxide nanoparticles supported onto oriented multi-walled carbon nanotube as electrodes for electrochemical capacitors. *Electrochim Acta* 298:468–483
12. Harilal M, Vidyadharan B, Misnon II, Anilkumar GM, Lowe A, Ismail J, Yusoff MM, Jose R (2017) One-dimensional assembly of conductive and capacitive metal oxide electrodes for high-performance asymmetric supercapacitors. *ACS Appl Mater Interfaces* 9(12):10730–10742
13. Yi H, Wang H, Jing Y, Peng T, Wang X (2015) Asymmetric supercapacitors based on carbon nanotubes@ NiO ultrathin nanosheets core-shell composites and MOF-derived porous carbon polyhedrons with super-long cycle life. *J Power Sources* 285:281–290
14. Sun T, Liu X, Li Z, Ma L, Wang J, Yang S (2017) Graphene-wrapped CNT@ MoS_2 hierarchical structure: synthesis, characterisation and electrochemical application in supercapacitors. *New J Chem* 41(15):7142–7150
15. Long H, Guo C, Wei G, Jiang L, Yu Y (2019) Facile synthesis of various carbon nanotube/metal oxide nanocomposites with high quality. *Vacuum* 166:147–150
16. Najib S, Erdem E (2019) Current progress achieved in novel materials for supercapacitor electrodes: mini review. *Nanoscale Adv* 1(8):2817–2827
17. Sahebani S, Zebarjad SM, Khaki JV, Lazzeri A (2016) The decoration of multi-walled carbon nanotubes with nickel oxide nanoparticles using chemical method. *Int Nano Lett* 6(3):183–190
18. Tang X, Liang M, Zhang Y, Sun W, Wang Y (2019) Ultrafine ternary metal oxide particles with carbon nanotubes: a metal-organic-framework-based approach and superior lithium-storage performance. *Dalton Trans* 48(13):4413–4419
19. Fisher RA, Watt MR, Ready WJ (2013) Functionalized carbon nanotube supercapacitor electrodes: a review on pseudocapacitive materials. *ECS J Solid State Sci Technol* 2(10):M3170–M3177
20. Arunachalam R, Prataap RV, Pavul Raj R, Mohan S, Vijayakumar J, Péter L, Al Ahmad M (2019) Pulse electrodeposited RuO_2 electrodes for high-performance supercapacitor applications. *Surf Eng* 35(2):102–108
21. Wang YT, Lu AH, Zhang HL, Li WC (2011) Synthesis of nanostructured mesoporous manganese oxides with three-dimensional frameworks and their application in supercapacitors. *J Phys Chem C* 115(13):5413–5421
22. Yin Y, Zeng H, Sui Q, Xiang C, Zou Y, Chu H, Qiu S, Chen Q, Xu F, Sun L (2019) Formation of CoO-NiO nanoparticles on nitrogen doped porous carbon as high performance supercapacitor electrode. *Int J Electrochem Sci* 14(1):764–776
23. Li T, Yu H, Zhi L, Zhang W, Dang L, Liu Z, Lei Z (2017) Facile electrochemical fabrication of porous Fe_2O_3 nanosheets for flexible asymmetric supercapacitors. *J Phys Chem C* 121(35):18982–18991
24. Sk MM, Yue CY, Ghosh K, Jena RK (2016) Review on advances in porous nanostructured nickel oxides and their composite electrodes for high-performance supercapacitors. *J Power Sources* 308:121–140
25. Xiao H, Yao S, Liu H, Qu F, Zhang X, Wu X (2016) NiO nanosheet assembles for supercapacitor electrode materials. *Prog Nat Sci Mater Int* 26(3):271–275
26. Ates M, Eker AA, Eker B (2017) Carbon nanotube-based nanocomposites and their applications. *J Adhes Sci Technol* 31(18):1977–1997
27. Yao M, Hu Z, Liu Y, Liu P, Ai Z, Rudolf O (2015) 3D hierarchical mesoporous rose-like NiO nanosheets for high-performance supercapacitor electrodes. *J Alloys Compd* 648:414–418
28. Lv J, Wang Z, Miura H (2018) Facile synthesis of mesoporous NiO nanoflakes on graphene foam and its electrochemical properties for supercapacitor application. *Solid State Commun* 269:45–49
29. Hui X, Qian L, Harris G, Wang T, Che J (2016) Fast fabrication of NiO@ graphene composites for supercapacitor electrodes: combination of reduction and deposition. *Mater. Des* 109:242–250
30. Lin J, Jia H, Liang H, Chen S, Cai Y, Qi J, Qu C, Cao J, Fei W, Feng J (2018) In situ synthesis of vertical standing nanosized NiO encapsulated in graphene as electrodes for high-performance supercapacitors. *Adv Sci* 5(3):1700687
31. Adekunle AS, Ozoemena KI, Mamba BB, Agboola BO, Oluwatobi OS (2011) Supercapacitive properties of symmetry and the asymmetry two electrode coin type supercapacitor cells made from MWCNTs/nickel oxide nanocomposite. *Int J Electrochem Sci* 6:4760–4774
32. Feng Y, Zhang H, Li W, Fang L, Wang Y (2016) Targeted synthesis of novel hierarchical sandwiched NiO/C arrays as high-efficiency lithium ion batteries anode. *J Power Sources* 301:78–86
33. Shi S, Wan G, Wu L, He Z, Wang K, Tang Y, Xu X, Wang G (2019) Ultrathin manganese oxide nanosheets uniformly coating on carbon nanocoils as high-performance asymmetric supercapacitor electrodes. *J Colloid Interface Sci* 537:142–150
34. Li X, Yu L, Wang G, Wan G, Peng X, Wang K, Wang G (2017) Hierarchical NiAl LDH nanotubes constructed via atomic layer deposition assisted method for high performance supercapacitors. *Electrochim Acta* 255:15–22
35. Yu L, Wan G, Peng X, Dou Z, Li X, Wang K, Lin S, Wang G (2016) Fabrication of carbon-coated NiO supported on graphene for high performance supercapacitors. *RSC Adv* 6(17):14199–14204
36. Yu L, Wang G, Wan G, Wang G, Lin S, Li X, Wang K, Bai Z, Xiang Y (2016) Highly effective synthesis of NiO/CNT nanohybrids by atomic layer deposition for high-rate and long-life supercapacitors. *Dalton Trans* 45(35):13779–13786
37. Yu W, Li BQ, Ding SJ (2016) Electroless fabrication and supercapacitor performance of CNT@ NiO-nanosheet composite nanotubes. *Nanotechnology* 27(7):075605
38. Dai K, Liang C, Dai J, Lu L, Zhu G, Liu Z, Liu Q, Zhang Y (2014) High-yield synthesis of carbon nanotube-porous nickel oxide nanosheet hybrid and its electrochemical capacitance performance. *Mater Chem Phys* 143(3):1344–1351
39. Vijayakumar S, Ponnalagi AK, Nagamuthu S, Muralidharan G (2013) Microwave assisted synthesis of Co_3O_4 nanoparticles for high-performance supercapacitors. *Electrochim Acta* 106:500–505
40. Wang F, Zhou Q, Li G, Wang Q (2017) Microwave preparation of 3D flower-like $\text{MnO}_2/\text{Ni}(\text{OH})_2$ /nickel foam composite for high-performance supercapacitors. *J Alloys Compd* 700:185–190
41. Kumar RD, Andou Y, Sathish M, Karuppachamy S (2016) Synthesis of nanostructured CuWO_3 and CuWO_4 for supercapacitor applications. *J Mater Sci Mater Electron* 27(3):2926–2932
42. Kumar RD, Andou Y, Karuppachamy S (2016) Microwave-assisted synthesis of Zn- WO_3 and ZnWO_4 for pseudocapacitor applications. *J Phys Chem Solids* 92:94–99
43. Zeng S, Cao Y, Sang W, Li T, Gan N, Zheng L (2012) Enrichment of polychlorinated biphenyls from aqueous solutions using Fe_3O_4 grafted multiwalled carbon nanotubes with poly dimethyl diallyl ammonium chloride. *Int J Mol Sci* 13(5):6382–6398
44. Zhu G, Liu Y, Xi C, Bao C, Xu H, Shen X, Zhu X (2013) Polymer guided synthesis of Ni(OH)₂ with hierarchical structure and their

- application as the precursor for sensing materials. *Cryst Eng Comm* 15(44):9189–9195
45. Banerjee D, Ghorai UK, Das NS, Das B, Thakur S, Chattopadhyay KK (2018) Amorphous carbon nanotubes–nickel oxide nanoflower hybrids: a low cost energy storage material. *ACS Omega* 3(6):6311–6320
 46. Basavegowda N, Mishra K, Lee YR (2019) Fe₃O₄-decorated MWCNTs as an efficient and sustainable heterogeneous nanocatalyst for the synthesis of polyfunctionalised pyridines in water. *Mater Technol* 34:558–569
 47. Ngo YL, Hur SH (2016) Low-temperature NO₂ gas sensor fabricated with NiO and reduced graphene oxide hybrid structure. *Mater Res Bull* 84:168–176
 48. Qiu Z, He D, Wang Y, Zhao X, Zhao W, Wu H (2017) High performance asymmetric supercapacitors with ultrahigh energy density based on hierarchical carbon nanotubes@ NiO core–shell nanosheets and defect-introduced graphene sheets with hole structure. *RSC Adv* 7(13):7843–7856
 49. Liu W, Lu C, Wang X, Liang K, Tay BK (2015) In situ fabrication of three-dimensional, ultrathin graphite/carbon nanotube/NiO composite as binder-free electrode for high-performance energy storage. *J Mater Chem A* 3(2):624–633
 50. Kim DK, Hwang M, Ko D, Kang J, Seong KD, Piao Y (2017) Electrochemical performance of 3D porous Ni-Co oxide with electrochemically exfoliated graphene for asymmetric supercapacitor applications. *Electrochim Acta* 246:680–688
 51. Ali MA, Solanki PR, Srivastava S, Singh S, Agrawal VV, John R, Malhotra BD (2015) Protein functionalized carbon nanotubes-based smart lab-on-a-chip. *ACS Appl Mater Interfaces* 7(10):5837–5846
 52. Wu Q, Wen M, Chen S, Wu Q (2015) Lamellar-crossing-structured Ni(OH)₂/CNTs/Ni(OH)₂ nanocomposite for electrochemical supercapacitor materials. *J Alloys Compd* 646:990–997
 53. Roy A, Ray A, Saha S, Ghosh M, Das T, Satpati B, Nandi M, Das S (2018) NiO-CNT composite for high performance supercapacitor electrode and oxygen evolution reaction. *Electrochim Acta* 283:327–337
 54. Wu C, Deng S, Wang H, Sun Y, Liu J, Yan H (2014) Preparation of novel three-dimensional NiO/ultrathin derived graphene hybrid for supercapacitor applications. *ACS Appl Mater Interfaces* 6(2):1106–1112
 55. Hakamada M, Abe T, Mabuchi M (2016) Electrodes from carbon nanotubes/NiO nanocomposites synthesised in modified Watts bath for supercapacitors. *J Power Sources* 325:670–674
 56. Bouessay I, Rougier A, Tarascon JM (2004) Electrochemically inactive nickel oxide as electrochromic material. *J Electrochem Soc* 151(6):H145–H152
 57. Ren B, Fan M, Yang X, Wang L, Yu H (2019) 3D hierarchical structure electrodes of MnO₂ nanosheets decorated on needle-like NiCo₂O₄ nanocones on Ni foam as a cathode material for asymmetric supercapacitors. *Chem Sel* 4(19):5641–5650
 58. Zheng YZ, Ding HY, Zhang ML (2009) Preparation and electrochemical properties of nickel oxide as a supercapacitor electrode material. *Mater Res Bull* 44(2):403–407
 59. Xu J, Li L, He F, Lv R, Yang P (2014) A novel double-shelled C@NiO hollow microspheres: synthesis and application for electrochemical capacitor. *Electrochim Acta* 148:211–219
 60. Shin DH, Lee JS, Jun J, Jang J (2014) Fabrication of amorphous carbon-coated NiO nanofibers for electrochemical capacitor applications. *J Mater Chem A* 2(10):3364–3371
 61. Iqbal N, Wang X, Babar AA, Yu J, Ding B (2016) Highly flexible NiCo₂O₄/CNTs doped carbon nanofibers for CO₂ adsorption and supercapacitor electrodes. *J Colloid Interface Sci* 476:87–93
 62. Jiang Y, Leng X, Jia Z, Chen H, Suo H, Zhao C (2015) In situ growth of NiO nanostructures directly on nickel foam and its electrochemical property. *J Mater Sci Mater Electron* 26(5):2995–3000
 63. Nathan T, Aziz A, Noor AF, Prabakaran SR (2008) Nanostructured NiO for electrochemical capacitors: synthesis and electrochemical properties. *J Solid State Electrochem* 12(7–8):1003–1009
 64. Kolathodi MS, Palei M, Natarajan TS (2015) Electrospun NiO nanofibers as cathode materials for high performance asymmetric supercapacitors. *J Mater Chem A* 3(14):7513–7522
 65. Su AD, Zhang X, Rinaldi A, Nguyen ST, Liu H, Lei Z, Lu L, Duong HM (2013) Hierarchical porous nickel oxide–carbon nanotubes as advanced pseudocapacitor materials for supercapacitors. *Chem Phys Lett* 561:68–73
 66. Lee JY, Liang K, An KH, Lee YH (2005) Nickel oxide/carbon nanotubes nanocomposite for electrochemical capacitance. *Synth Met* 150(2):153–157
 67. Zheng Y, Zhang M, Gao P (2007) Preparation and electrochemical properties of multiwalled carbon nanotubes–nickel oxide porous composite for supercapacitors. *Mater Res Bull* 42(9):1740–1747
 68. Zhang Y, Gui Y, Wu X, Feng H, Zhang A, Wang L, Xia T (2009) Preparation of nanostructures NiO and their electrochemical capacitive behaviors. *Int J Hydrog Energy* 34(5):2467–2470
 69. Zhu YG, Cao GS, Sun CY, Xie J, Liu SY, Zhu TJ, Zhao XB, Yang HY (2013) Design and synthesis of NiO nanoflakes/graphene nanocomposite as high performance electrodes of pseudocapacitor. *RSC Adv* 3(42):19409–19415
 70. Patil UM, Salunkhe RR, Gurav KV, Lokhande CD (2008) Chemically deposited nanocrystalline NiO thin films for supercapacitor application. *Appl Surf Sci* 255(5):2603–2607
 71. Xing W, Li F, Yan ZF, Lu GQ (2004) Synthesis and electrochemical properties of mesoporous nickel oxide. *J Power Sources* 134(2):324–330
 72. Zhu J, Jiang J, Liu J, Ding R, Ding H, Feng Y, Wei G, Huang X (2011) Direct synthesis of porous NiO nanowall arrays on conductive substrates for supercapacitor application. *J Solid State Chem* 184(3):578–583
 73. Chang HY, Chang HC, Lee KY (2013) Characteristics of NiO coating on carbon nanotubes for electric double layer capacitor application. *Vacuum* 87:164–168

Publisher's note Springer Nature remains neutral with regard to jurisdictional claims in published maps and institutional affiliations.